Global and Planetary Change 100 (2013) 109–118

Contents lists available at SciVerse ScienceDirect

Global and Planetary Change

journal homepage: www.elsevier.com/locate/gloplacha

A large-scale coherent signal of canopy status in maximum latewood density of tree rings at arctic treeline in North America

Pieter S.A. Beck [a,*], Laia Andreu-Hayles [b,c], Rosanne D'Arrigo [b], Kevin J. Anchukaitis [b,d], Compton J. Tucker [e], Jorge E. Pinzón [e], Scott J. Goetz [a]

[a] Woods Hole Research Center, 149 Woods Hole Road, Falmouth, MA 02540, USA
[b] Tree-Ring Laboratory, Lamont-Doherty Earth Observatory of Columbia University, 61 Route 9W, Palisades, NY 10964, USA
[c] Institut Català de Ciències del Clima (IC3), C/ Dr Trueta 203, 08005 Barcelona, Catalonia, Spain
[d] Woods Hole Oceanographic Institution, Woods Hole, MA 02542, USA
[e] Biospheric Science Branch, NASA Goddard Space Flight Center, Greenbelt, MD 20771, USA

ARTICLE INFO

Article history:
Received 1 May 2012
Accepted 4 October 2012
Available online 13 October 2012

Keywords:
boreal forest
arctic tundra
high latitudes
Normalized Difference Vegetation Index
remote sensing
tree ring

ABSTRACT

We compared tree-ring width (TRW) and maximum latewood density (MXD) chronologies to remotely sensed indices of productivity (NDVI) and snowmelt since 1981 and to the instrumental temperature record at four arctic treeline sites in North America. Our results show that at these sites, TRW chronologies reflect temperatures less consistently than the MXD chronologies do and that the NDVI does not correlate significantly with TRW at high-frequency, i.e. when comparing yearly values. In contrast, the MXD chronologies correlate positively and significantly with NDVI and temperature during the growing season at all sites. Neither TRW or MXD chronologies appeared consistently influenced by the annual timing of snowmelt. A comparison of tree-ring chronologies and temperatures since 1900 confirms that MXD has tracked growing season temperature at these treeline sites throughout the past century. A spatial evaluation of the correlations further reveals that each of the MXD chronologies investigated here reflects interannual variation in NDVI and growing season temperatures across a large geographic region. As a result, they collectively provide a spatially comprehensive record of historic early-season canopy status as well as growing season temperatures for the high latitudes of North America.

1. Introduction

Higher northern latitudes are experiencing the greatest degree of climate warming on the globe today, and northern ecosystems are projected to undergo substantial change in the coming century (ACIA, 2004). Reconstructions of historic tree distribution suggest that vegetation at high northern latitudes can respond abruptly and non-linearly to climate change (Lloyd et al., 2003; MacDonald et al., 2008) and a northward expansion of forests into present tundra areas is predicted by global vegetation models under future climate scenarios (Lucht et al., 2006; Scholze et al., 2006). If such changes take place over large areas of the Arctic, they will dramatically alter global carbon cycling, land-atmosphere energy exchange, biodiversity patterns, and ecosystem functioning (Bonan, 2008). Therefore, the responses of tundra and boreal ecosystems to current and future climate variability need to be better understood, and in this context, trees growing at the forest–tundra transition, i.e. at arctic treeline, are of particular interest.

Tree-ring data from treeline sites have often been used for climate reconstructions because, in such settings, tree growth is primarily limited by climate, and at arctic treeline specifically by temperature, rather than by biotic factors such as stand dynamics (e.g. Cook and Kairiukstis, 1990). Tree-ring records of annual tree-ring width (TRW) and maximum latewood density (MXD) have proven to be useful proxies of growing season temperatures (Briffa et al., 1995; Jacoby and D'Arrigo, 1995). However, there are reports from a number of sites, mainly at high latitudes, that some metrics of tree growth, and tree-ring widths in particular, have increasingly diverged from temperature in recent decades (Briffa et al., 1998a, 1998b; Wilmking et al., 2004; D'Arrigo et al., 2008, 2009; Andreu-Hayles et al., 2011). Several causes for this loss of temperature sensitivity in tree-ring chronologies have been proposed (Esper and Frank, 2009), most notably a shift from temperature-limitation to moisture-limitation on tree growth (e. g. Jacoby and D'Arrigo, 1995; Barber et al., 2000; D'Arrigo et al., 2004a, 2004b, 2008, 2009; Beck et al., 2011a; Juday and Alix, 2012) and progressively delayed snowmelt reducing the annual period in which tree growth is most sensitive to temperatures (Vaganov et al., 1999).

Meteorological data recorded at weather stations are commonly used to evaluate tree ring records as climate proxies. Remote sensing data from Earth-orbiting satellites now provide a nearly 30-year record of the Normalized Difference Vegetation Index (NDVI), a landscape-level proxy for primary productivity (Myneni et al., 1997; Goetz et al., 2005; Pinzon et al., submitted for publication). This globally mapped vegetation index

* Corresponding author at: Woods Hole Research Center, 149 Woods Hole Road, Falmouth, MA 02540, USA. Tel.: +1 508 444 1507; fax: +1 508 444 1807.
E-mail address: pbeck@whrc.org (P.S.A. Beck).

0921-8181/$ – see front matter
http://dx.doi.org/10.1016/j.gloplacha.2012.10.005

therefore provides the unique opportunity to evaluate the extent to which small-scale records of tree physiology in tree rings reflect not only variations in climate, but also in landscape or regional vegetation productivity. Furthermore, robust links between the satellite and tree-ring data resulting from such an evaluation could inform large-scale spatial extrapolations of historical tree-ring attributes from the dendrochronological record.

In interior Alaska, NDVI data support the growth decline observed over the last decades in spruce tree-ring records (Beck et al., 2011a). Similarly, Lloyd et al. (2010) showed that patterns of increasing and decreasing tree growth along a latitudinal gradient in Siberia match the fraction of the landscape showing positive and negative trends in summer NDVI, respectively. In a tundra area of Western Siberia, Forbes et al. (2009), and more recently Macias-Fauria et al. (2012), reported significantly positive correlations between NDVI in July and growth of shrubs determined from their ring widths. However, comparisons of tree rings to remotely sensed vegetation indices are still not abundant, and close to treeline, reported correlations of annual TRW of trees and NDVI can be low or non-significant (D'Arrigo et al., 2000; Kaufmann et al., 2004; Berner et al., 2011). While growth of mature spruce trees as well as NDVI has increased since 1982 in an ecotonal forest zone in Western Alaska, the high-frequency, i.e. year-to-year, changes in NDVI over this period were not consistently correlated with high-frequency changes in tree-ring widths (Beck et al., 2011a). Furthermore, Berner et al. (2011) documented cases of decreasing tree-ring widths in areas of increasing summer NDVI near treeline in northern Russia. In the latter case, the lack of agreement between the two metrics was attributed to low spatial density of tree cover in the study area. This potentially caused the NDVI data, which represents a spatially integrated measure, to reflect the canopy status of both trees and understory vegetation rather than tree productivity alone (Bunn and Goetz, 2006).

MXD chronologies often reflect current-year environmental conditions better than TRW chronologies do, because MXD appears to be less influenced by temperatures of previous years than TRW is (Frank and Esper, 2005; Andreu-Hayles et al., 2011). As a result, we hypothesized that high-frequency variation in MXD chronologies corresponded better to interannual variation in gross photosynthesis, as observed by NDVI. This hypothesis has not yet been extensively tested: D'Arrigo et al. (2000) found that MXD correlated positively with NDVI-derived net primary productivity over a relatively short period (i.e. <10 years) at three boreal sites, but did not investigate corresponding TRW series. More recently, Andreu-Hayles et al. (2011) demonstrated that NDVI over a 21-year period was correlated to MXD as well as TRW at a treeline site in northeastern Alaska, although during different times of the growing season.

Reconciling satellite observations and tree ring measurements at treeline would improve our understanding of the response of the treeline zone, and high latitude ecosystems in general, to past as well as future climate change. Therefore, we evaluated whether productivity indices extracted from tree rings and NDVI observations coherently describe the response of trees at the arctic treeline to recent climate variability. More precisely, we quantified how TRW and MXD chronologies at four treeline sites at high latitudes of western North America relate to the NDVI, snowmelt, and temperature records over the past three decades. We then extended the comparison between temperature and tree-ring data to most of the 20th century, and mapped the geographic extent of temperature and canopy status signals in the chronologies, in order to assess the temporal and spatial consistency of tree growth responses to climate variables.

2. Material and methods

2.1. Tree rings

Living and relict white spruce wood was sampled during the past decade and tree-ring chronologies (TRW and MXD) were developed for four locations near arctic treeline along a west–east gradient across Alaska and western Canada. The Seward Peninsula chronologies span the years 1389–2001 and were developed from collections made in 2002 at 14 sites at or near elevational treeline sites near the Tubutulik River (53 series, 65.1–65.2°N, 162.2°W, D'Arrigo et al., 2004a, 2005). The Firth River chronologies span 1067–2002 for TRW and 1073–2002 for MXD and were developed from samples collected at northern treeline at the Firth River in northwestern Alaska (232 series, 68.78°N, 142.35°W, Andreu-Hayles et al., 2011; Anchukaitis et al., in press). The Coppermine River chronologies span 1046–2003 for TRW and 1551–2003 for MXD and were developed for sites near the Coppermine River in the Northwest Territories, Canada (427 TRW series, 44 MXD series, 67.23°N, 115.92°W, D'Arrigo et al., 2009). Finally, the Thelon River chronologies span 1309–2004 for TRW and 1492–2004 for MXD and were developed from samples collected at the Thelon River near the border of the Northwest Territories and Nunavut, and is the easternmost of the four sites included here (86 TRW series, 183 MXD series, 64.03°N, 103.87°W, D'Arrigo et al., 2009). None of the sites had visible signs of recent fire or insect disturbance.

Individual raw TRW and MXD series were detrended using the Signal Free method (SF, Melvin and Briffa, 2008). After standardization and detrending, the individual series were combined into site-level chronologies using the biweight robust mean (Cook and Kairiukstis, 1990). The Signal Free method's ability to potentially mitigate 'trend distortion' and end effects that other standardization techniques may introduce motivated its application in this study of recent decades, when satellite and temperature data are available for comparison. Although high-frequency variation in chronologies is generally unaffected by the standardization procedure used, we also performed nine alternative procedures to ensure that the comparisons between tree-ring data and satellite or temperature data were not an artifact of the chosen treatment of the raw series. These alternative detrending and standardization methods included the standardized, and residual (autoregressive-standardized) chronologies produced after negative exponential (NEXP), regional curve standardization (RCS_PT, Cook and Kairiukstis, 1990; Cook and Peters, 1997; Helama et al., 2004), and 120-year 50% spline detrending (Cook and Peters, 1981).

2.2. Satellite data

We used the Global Inventory Modeling and Mapping Studies (GIMMS, version G) which is produced twice-monthly at 0.072° (~64 km^2) spatial resolution (Tucker et al., 2005) from data that the NOAA-Advanced Very High Resolution Radiometers (AVHRRs) have been acquiring since mid-1981. The spatio-temporal changes described by the GIMMS–NDVI since 2000 in the boreal zone of North America are consistent with those described by the more modern Moderate Resolution Imaging Spectroradiometers (Beck and Goetz, 2011). Globally, the GIMMS–NDVI captures vegetation's photosynthetic capacity best among other legacy (i.e. >25 years long) NDVI data sets (Beck et al., 2011b). Nonetheless, to prevent any potential idiosyncrasies in version G of the GIMMS–NDVI data from influencing the results, the analyses were repeated using a forthcoming version of the data set (version 3 g, Pinzon et al., submitted for publication).

Annual dates of snowmelt were mapped from version 3 and the version 3.1 update of Weekly Northern Hemisphere EASE-Grid Snow Cover data (http://nsidc.org/data/nsidc-0046.html, Armstrong and Brodzik, 2005). While these data are mapped on a 25 km grid, their actual spatial resolution is ~200 km. For each grid cell, snowmelt was initially assigned to the first snow-free date of the year. However, if that date was immediately followed by a snow-cover observation the next week, snowmelt was assigned to the next date without snow cover instead. This approach ignores any short snow-free periods in winter and unseasonably late snowfall events which are unlikely to cause a long-lasting snow pack. Instead, it quantifies the timing of the main spring transition from a snow-covered to a snow-free landscape.

2.3. Satellite - tree rings - climate data comparisons

Comparisons of tree-ring chronologies and NDVI since 1981 were complemented with comparisons of tree-ring chronologies and temperature and snowmelt over the same period. For this, a 1981–2008 monthly temperature data set, spatially aligned with the GIMMS–NDVI grid, was produced by McKenney et al. (2006). The climate grids were created by fitting statistically smoothed surfaces, using thin plate smoothing splines, to climate station data while estimating effects of latitude, longitude as well as elevation. Station data were collected from the National Climate Data Center in the U.S.A. and from the Meteorological Service of Canada. From both the GIMMS–NDVI and the meteorological gridded data sets, the four time series that coincided with the locations of the tree-ring sites were extracted (Fig. 1).

For each site, high-frequency signals in the chronologies, satellite data, and temperature data were compared by computing the correlations between yearly values in the TRW and MXD chronologies on the one hand, and monthly values of NDVI and maximum daily temperature since July 1981 on the other. These correlations were calculated with fortnightly frequency for the NDVI, and with monthly frequency for the meteorology data. In the case of NDVI, correlations were only calculated when observations were available in at least 12 years. At each site, chronologies were also compared to corresponding annual estimates of snowmelt since 1968.

For a longer-term perspective on the high-frequency agreement between tree-ring chronologies and temperatures, we also used a coarser resolution gridded temperature data set with 0.5° grid cells for the 20th century (CRU TS 3.1, Mitchell and Jones, 2005). Correlations between the chronologies and yearly CRU TS 3.1 temperatures since 1901 were calculated for each month using a 21-year sliding-window to ensure minimal influence of medium- or low-frequency variation.

We mapped the spatial reach of any productivity or climate signal registered in both the TRW and the MXD chronologies, using the correlation between the chronologies on the one hand, and the individual grid-cell level time series contained in the NDVI, climate, or snowmelt data sets, on the other. Maps of the chronology–NDVI and chronology–temperature correlations were produced for the months when the site-level analyses indicated a significant correlation between the

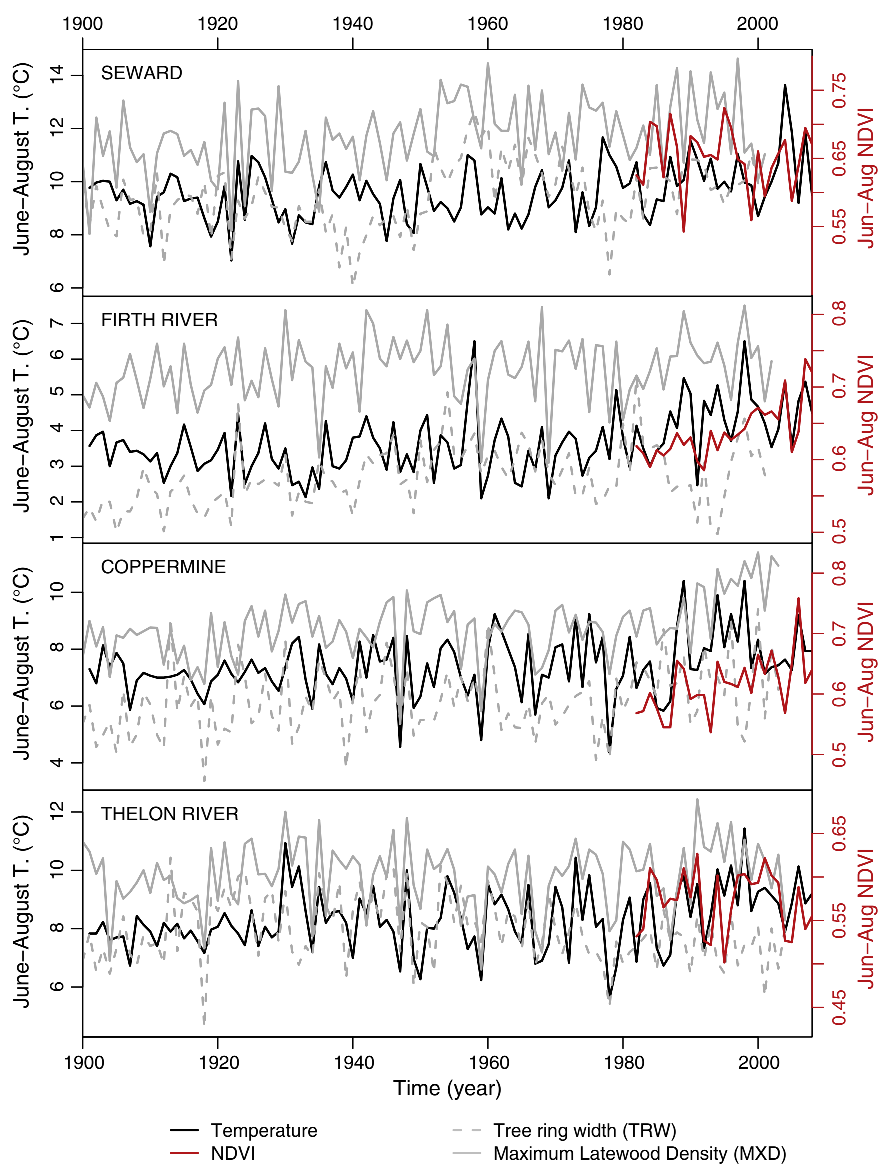

Fig. 1. Time series of June–August mean temperatures (CRU TS 3.1 0.5, Mitchell and Jones, 2005), June–August mean GIMMS NDVI, and chronologies of ring width and maximum latewood density processed using the Signal Free method (SF, Melvin and Briffa, 2008) for four treeline sites in Western North America. We note that the correlations between chronologies, temperatures, and NDVI vary between sites and months.

gridded data and the chronologies. When none of the months showed a consistent agreement with NDVI, maps were produced for July. The Pearson's product moment correlation coefficient was used as a measure of agreement.

3. Results

TRW chronologies did not show a consistent pattern of agreement with NDVI during any time of the year since 1981. In contrast, MXD chronologies correlated positively and statistically significantly ($P<0.05$) with the NDVI measured over the sites at the start of the growing season (Fig. 2). NDVI showed a statistically significant correlation with MXD earlier in the year at the Seward and Firth River sites, than it did at the Coppermine and Thelon River sites (in April–May, and May–June, respectively, Fig. 2) where the growing season starts later, as measured by the annual spring increase in NDVI, temperature, and the timing of snowmelt (See Appendix A, Fig. A.1). The observed agreement between NDVI and MXD in the high-frequency domain isn't an artifact of detrending and standardization, as it is consistent across chronologies generated using the different methods and present when using the raw tree-ring data (Fig. A.2).

NDVI values in the spring–summer transition were higher when snowmelt occurred earlier and the timing of significant NDVI–snowmelt correlations reflected the East–west gradient of later spring across our sites: snowmelt correlated significantly ($P\leq0.1$) with NDVI in early May to early June at Seward ($r=-0.49$ to -0.54) in late May to late June at Firth River ($r=-0.43$ to -0.45), in early June at Thelon River ($r=-0.36$), and in early June to early July at Coppermine ($r=-0.45$ to -0.61).

Despite the apparent influence of the timing of snowmelt on NDVI at the start of the growing season, and NDVI partly accounting for interannual variation in MXD, observed correlations between MXD and snowmelt were low and statistically insignificant ($|r|\leq0.26$, $P_r\geq0.1$, $N=34$–37). When restricting the comparison to the years with NDVI data, i.e. post 1981, MXD showed a negative response to later snowmelt at the Firth river site ($r=-0.53$, $P=0.01$, $N=21$), but not at the three other sites ($-0.13\leq r\leq-0.08$, $P\geq0.6$, $N=20$-23). At none of the sites did the date of snowmelt explain variance in MXD, beyond that explained by NDVI at the start of the growing season (SOG), as measured by the correlations between snowmelt and the residuals of the linear regression $MXD=a*NDVI_{SOG}+b$ ($|r|\leq0.3$, $P\geq0.2$, $N=20$–23). At the Firth river, the only site where snowmelt did explain a significant amount of variance in MXD, but only since 1982, $NDVI_{SOG}$ did not explain the residual variance of the linear regression $MXD=a*snow\_melt+b$ ($r=0.28$, $P=0.22$, $N=21$).

Over the 21–24 year periods when both NDVI and tree-ring data were available, TRW did not consistently respond to temperature whereas MXD values correlated positively and significantly with temperature throughout the growing season at all sites (Fig. 2). Using the CRU TS 3.1 data set (Mitchell and Jones, 2005), rather than the shorter but higher resolution temperature data set, confirmed the observed difference between high-frequency TRW-temperature and MXD-temperature relationships over the 1981–2002 period (Fig. 3). Moreover, extending this comparison in time to the 1901–2002 period using the CRU TS 3.1 data set indicated that the MXD series reflect high-frequency variation in summer temperatures at the treeline sites more consistently than the TRW series do throughout the 20th century.

Site-level MXD chronologies correlated with NDVI as well as temperatures across relatively large geographical regions surrounding the field sampling sites at the start of the growing season (Fig. 4). The absence of significant correlations between TRW chronologies and temperatures or NDVI observed at the site level was also reflected in the correlation maps (Fig. A.3). Similarly, maps indicated a lack of a consistent relationship between snowmelt date and MXD or TRW (Fig. A.4). Nonetheless, MXD at the Coppermine and Thelon River sites showed a weakly negative correlation to snowmelt dates further north-east when considering the period since 1968. Substituting the GIMMS version 3 g NDVI data for the version G data, did not alter the observed patterns in temporal (Fig. A.5) or spatial (Fig. A.6) agreement between the remotely sensed vegetation indices and tree-ring chronologies.

4. Discussion

Tree-ring widths at the northern treeline sites studied here do not appear to robustly reflect temperatures of recent decades and are not

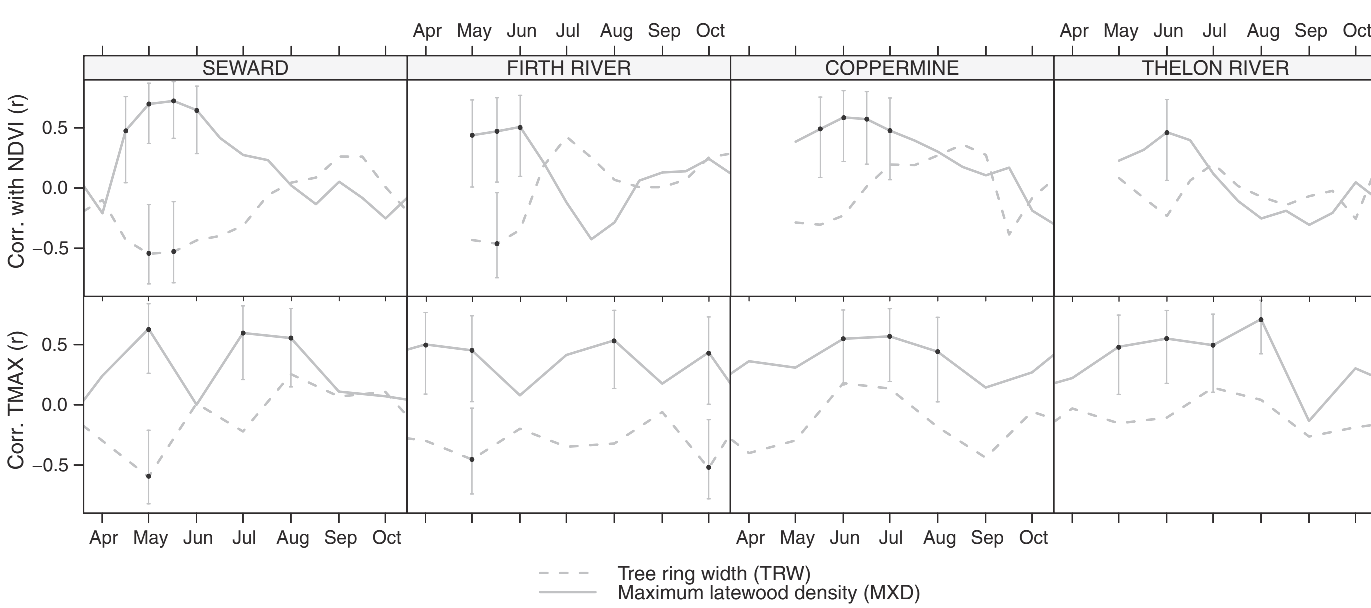

Fig. 2. Correlation (r) between tree-ring chronologies (ring width and maximum latewood density (MXD)) and (top row) corresponding GIMMS–NDVI observations resampled to monthly resolution and fortnightly frequency, and (bottom row) monthly means of daily maximum temperatures at four sites. Black dots indicate statistically significant correlations ($P<0.05$), and whiskers show the 95% confidence intervals around them. Correlations were calculated from time series starting in July 1981 and ending between 2001 and 2004 depending on the year of sampling at each site.

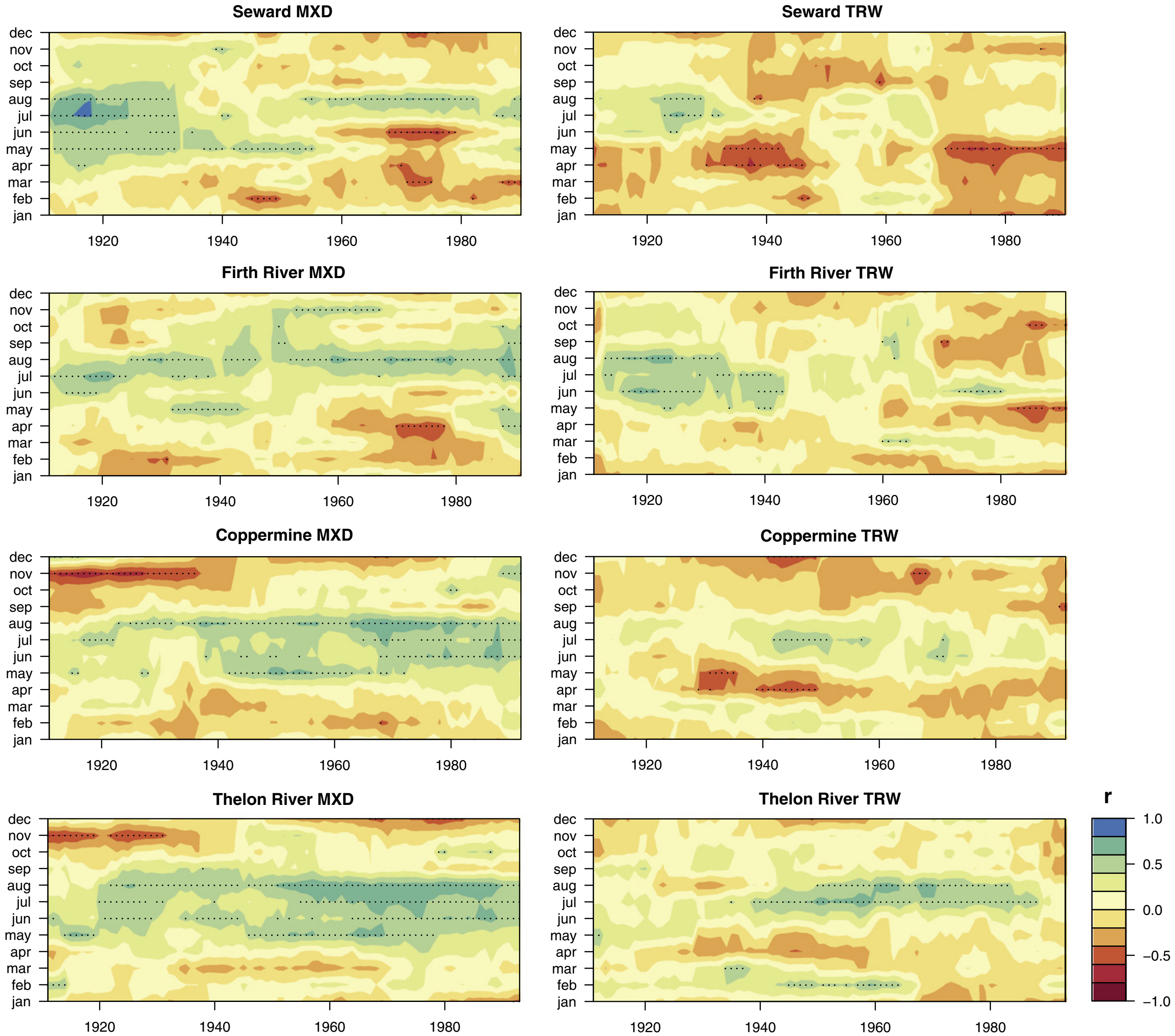

Fig. 3. Correlations between maximum latewood density (MXD) and tree-ring width (TRW) chronologies and mean temperatures in individual months over 21 year periods since 1901. Temperature data were extracted from a gridded data set (CRU TS 3.1, Mitchell and Jones, 2005) and black dots represent statistically significant correlations ($P<0.05$).

well-represented by the available coincident NDVI data. This suggests that, unlike in areas of high tree density in interior Alaska (Beck et al., 2011a), the NDVI is not a good indicator of radial tree growth measured by ring widths at these ecotonal sites characterized by marginal tree cover. Contrasting effects of changing environmental conditions on understory tundra vegetation communities, which dominate the satellite signal at treeline, and trees, whose growth-responses may depend on site-level factors (Wilmking et al., 2005), could also contribute to this mismatch. In contrast to TRW, MXD correlates consistently positively with temperatures as well as NDVI since 1981. As such, MXD reflects a response to year-to-year environmental variability that is consistent between tree physiology and landscape-level vegetation productivity, despite the role other vegetation plays in the latter. However, the MXD chronologies correlate significantly with the NDVI primarily at the start of the growing season, although they reflect temperatures over longer periods, beginning around the time of snowmelt (i.e. in April-May) and continuing through late summer (i.e. August, Fig. 2), as is typical for the MXD parameter. Therefore, the positive and statistically significant relationship between MXD and NDVI is unlikely to be the result of temperatures controlling gross photosynthesis (as quantified by NDVI) and MXD in identical ways.

MXD chronologies are fewer and thus provide a sparser global coverage than TRW chronologies do, amongst others because of the greater labor required to prepare wood for MXD measurements. In this context, it is remarkable that the four MXD chronologies from western to central high latitudes of North America analyzed here, collectively provide a comprehensive record of recent growing season temperatures and landscape-level productivity at the start of the growing season across this entire region (Fig. 4). The gridded surface climate data used here, like most regional data sets of historical climate, rely in large part on the interpolation of station data. As the cover of meteorological stations is sparse at high latitudes, the temperature data may theoretically underestimate the true variations in temperatures at finer spatial scales (McKenney et al., 2006). Any such unrealistic spatial autocorrelation

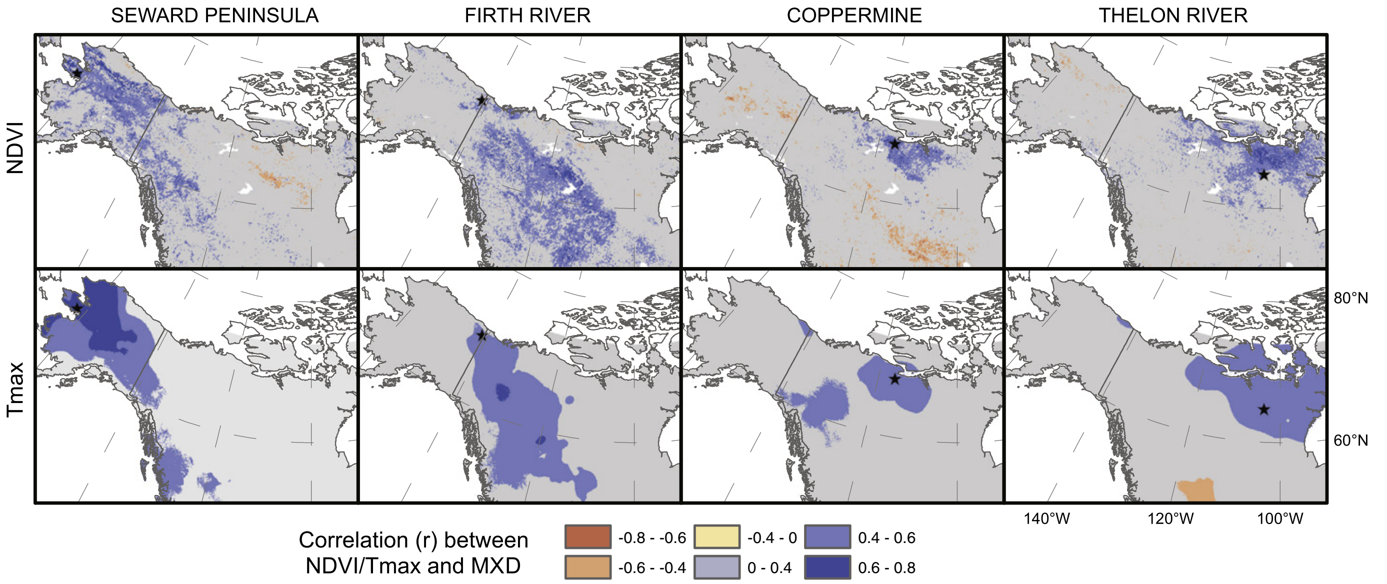

Fig. 4. Correlation (r) between maximum latewood density (MXD) tree-ring chronologies at four sites indicated by stars and (top row) GIMMS NDVI, and (bottom row) temperature at the start of the growing season. NDVI and mean daily maximum temperature in May was used at the Seward Peninsula and Firth River sites, and in June for the Coppermine and Thelon River sites where the growing season starts later, as measured by the spring increase in NDVI and temperature, and by the timing of snowmelt (Fig. A.1). Correlations were calculated from time series starting in 1982 and ending between 2001 and 2004 depending on the year of sampling at each site. Gray areas indicate non-significant correlation ($P \geq 0.05$).

in the climate data could introduce artifacts in the mapped correlations between ring chronologies and climate data. In particular, they could cause an over or under-estimation of the spatial domain over which ring chronologies document climate, depending on how well or poorly conditions at the collection site are reproduced by the available meteorological stations. Indeed, this is the reason why in the present study, chronologies were not compared to precipitation patterns, which, particularly in summer, vary at relatively fine spatial scales and therefore are often poorly reproduced by spatial climate models (McKenney et al., 2006). The GIMMS–NDVI data originate in satellite observations at 1.1 km resolution that are sampled to 4 km resolution onboard the satellite and later aggregated to ~8 km grid cells. Compared to the climate data, and over distances >~25 km, they are therefore practically void of spatial autocorrelation attributable to data processing and they realistically capture spatial variability in vegetation productivity at fine as well as coarse spatial resolution. We found that the geographically extensive correlations between MXD and temperatures (Fig. 4) were confirmed by the spatial pattern in MXD–NDVI correlations. They are therefore unlikely to be an artifact of the spatial interpolation used to generate the gridded temperature data sets. Instead, the satellite-derived NDVI data show how the MXD record reflects the large-scale spatial covariance of climate and ecosystem activity, and suggest that MXD chronologies can provide a robust and spatially comprehensive record of historic high-frequency variation in regional temperatures and associated vegetation productivity at North American high latitudes.

Early in the growing season, the NDVI showed a lagged response to warming. June NDVI reflected Tmax in the preceding month of April more strongly than Tmax in May or June, with respective correlations for observations averaged across the tree-ring sites: $r=0.66$, 0.47, 0.37 ($df=25$, 25, 25; $P=0.0002$, 0.01, 0.06). This represents a “ramping up” of photosynthetic activity and leaf development in response to accumulated heat (Bronson et al., 2009), and may explain why at the Firth and Thelon river sites temperature–MXD correlations become discernible earlier in the year (April–May) than NDVI–MXD correlations (May–June). However, at the Seward and Firth River sites in particular, the MXD chronologies have not reflected temperatures at the end of spring consistently through the second half of the 20th century (Fig. 3), suggesting that spring temperature is not a primary influence on MXD at least at these sites.

At northern tree line in North America, NDVI values in the spring and early summer reflect both the timing of snowmelt and vegetation productivity in the period around it, as snowmelt affects optical reflectance in ways that are similar to vegetation greening (Dye and Tucker, 2003). Vaganov et al. (1999) suggested, based on Eurasian chronologies, that the timing of snowmelt and the temperatures in the weeks after snowmelt, which also control photosynthesis (Bergeron et al., 2007), significantly influence MXD and TRW at the forest–tundra transition. Our results indicated that in North America, this is currently not the case for TRW, as TRW did not correlate with NDVI, temperatures, or snowmelt timing. MXD did show temporally and spatially robust correlations with temperatures and NDVI at the start of the growing season, but reflected snowmelt dates since 1982 only at the Firth River site. Over the period since 1968, interannual variation in MXD at the Coppermine and Thelon River was similar to that in snowmelt timing in adjacent tundra regions (Fig. A.4). The modest length of the NDVI record, as well as the covariance of snowmelt and NDVI at the start of the growing season, make it difficult to distinguish the influence of both on tree-ring metrics. That said, the much stronger and more consistent correlation between NDVI and MXD indicates that the latter reflects canopy status at the start of the growing season irrespective of the timing of snowmelt. Alternatively, the snow cover data used here, which are of coarser spatial (200 km vs. 8 km), but finer temporal resolution than the NDVI data (weekly vs. twice-monthly), might inadequately capture interannual snowmelt dynamics at the site-level. However, annual dates of snowmelt vary relatively homogenously across landscapes, despite local spatial variations in snow depth and timing of snowmelt due to topography and surface roughness amongst others (Sturm and Wagner, 2010). Moreover, significant correlations were observed at all sites between snowmelt and NDVI surrounding the period of snowmelt, despite scale discrepancies in the two data sets. This supports the notion that the snowmelt maps do indeed reflect site-level dynamics. Consequently, the lack of correlation between snow melt dates and MXD indicates that at arctic tree line in North America, MXD provides a proxy of canopy status at the start of the growing season, rather than of the date of snowmelt.

While MXD can be influenced by the radial dimension of tracheids (Kirdyanov et al., 2007), it is primarily a function of cell wall thickness in latewood (Yasue et al., 2000; Panyushkina et al., 2003). Unsurprisingly, the strongest climate signal in MXD at arctic treeline is often found in boreal summer (e.g. Davi et al., 2003; D'Arrigo et al. 2004a, 2009; Anchukaitis et al., in press), when the final latewood cells of the ring are produced and mature. Nonetheless, many of these tree-ring density chronologies do contain a secondary early growing season temperature signal as well (e.g. Briffa et al., 1992; Davi et al., 2003), as do the four North American MXD chronologies analyzed here. The precise mechanism by which temperatures, and particularly those at the end of boreal spring, might control latewood characteristics is not known. Temperature and NDVI covary early in the growing season, such that the correlation between MXD and early growing season canopy productivity shown here is not necessarily indicative of a physiological pathway linking photosynthesis early in the growing season to latewood cell growth. Given the strong controls of temperature on photosynthesis in the May and June period in our study area, our results instead are indicative of parallel, but independent, controls of spring temperatures on latewood development and photosynthesis. Finally, our findings indicate that later summer temperature controls on MXD are unlikely to be mediated by coeval canopy status, as later summer NDVI values did not correlate with MXD.

This study presents the first comparison of paired TRW and MXD chronologies with satellite-derived proxies of vegetation activity at multiple sites. We found that MXD chronologies from North American arctic tree line sites closely reflected growing season temperatures and canopy status at the start of the growing season measured over the last three decades. In this respect, the MXD chronologies contrast strongly with the TRW chronologies from the same sites, which did not show significant agreement with regional temperature or gross productivity variations at the landscape scale. Our findings indicate that, at least at arctic tree line in North America where white spruce is dominant, MXD records can be linked to regional vegetation productivity early in the growing season because they are both highly temperature-dependent. Further research is needed to investigate the robustness of this relationship across the pan-Arctic, and at alpine treeline, where TRW and MXD chronologies are also commonly used for climate reconstruction, but where other tree species dominate.

Acknowledgments

We acknowledge support from the National Science Foundation (0902051) to RDA, KJA, and (0902056) to SJG and PSAB, from the NOAA Carbon Cycle Science program (NA08OAR4310526) and NASA Carbon program (NNX08AG13G) to SJG, and the MICINN mobility grant and the Marie Curie International Outgoing Fellowship (PIOF-GA-2009-253277) awarded to LAH. The authors thank Brendan and Chris Buckley, and Erika Mashig for field work, Ashley Curtis, Anna Verstege, and David Frank for building tree-ring chronologies, Ed Cook for access to the signal free standardization code, Greg Fiske and Logan Berner for data processing, and Dan McKenney for producing GIMMS-compatible climate surfaces.

Appendix A

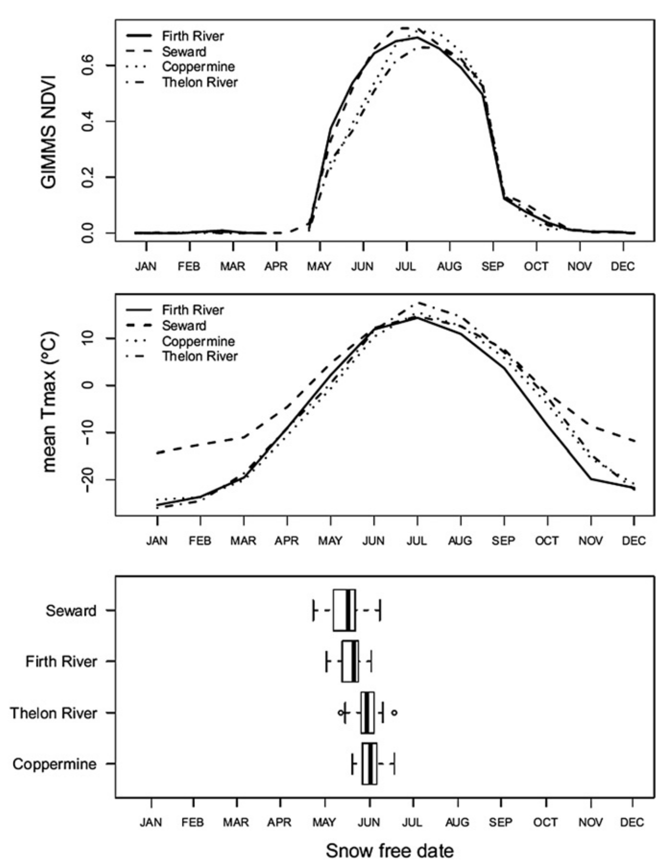

Fig. A.1. (Top) Mean fortnightly GIMMS–NDVI over the period 1982–2008 and (middle) monthly means of daily maximum temperature (Tmax), as well as (bottom) the timing of snow melt between 1982 and 2006 at the four sites where tree rings were collected.

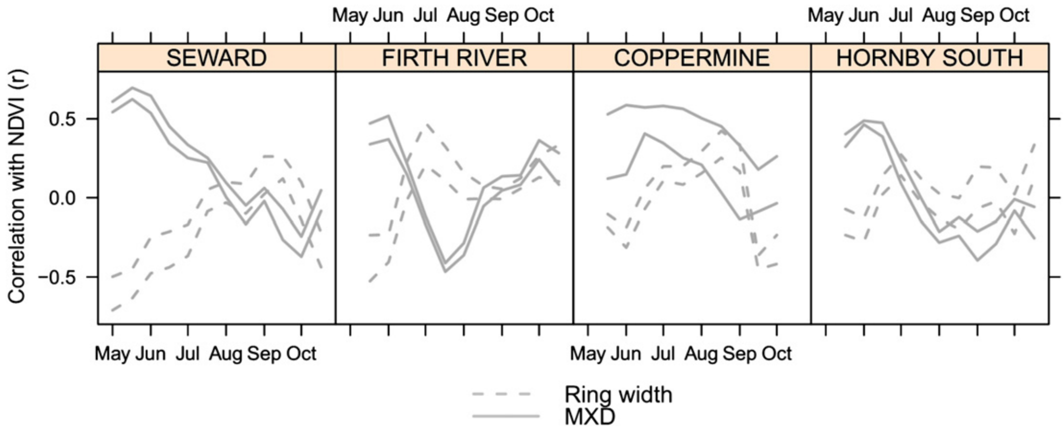

Fig. A.2. Range in correlations (r) between GIMMS–NDVI observations resampled to monthly resolution and fortnightly frequency, and raw tree-ring data as well as chronologies generated using 10 different detrending and standardization methods. Correlations were calculated from time series starting in July 1981 and ending between 2001 and 2004 depending on the year of sampling at each site. The 10 detrending and standardization methods comprise Signal Free processing (SF, Melvin and Briffa, 2008), and the standardized, residual and autoregressive(AR)-standardized chronologies produced after negative exponential (NEXP), regional curve standardization (RCS_PT, Cook and Kairiukstis, 1990; Cook and Peters, 1997; Helama et al., 2004), and 120-year 50% spline detrending (Cook and Peters, 1981).

References for Fig. A.2

Cook, E.R. and Kairiukstis, L.A. (Eds.), 1990. Methods of dendrochronology. Applications in the environmental sciences. Kluwer, Dordrecht, 394 pp.
Cook, E.R. and Peters, K., 1997. Calculating unbiased tree-ring indices for the study of climaticand environmental change. Holocene, 7, 359-368.
Cook, E.R. and Peters, K., 1981. The smoothing spline: a new approach to standardizing forest interior tree-ring width series for dendroclimatic studies. Tree-Ring Bulletin, 41, 45–53.
Helama, S., Lindholm, S., Timonen, M. and Eronen, M., 2004. Detection of climate signal indendrochronological data analysis: a comparison of tree-ring standardization methods. Theoretical and Applied Climatology, 79, 239-254.
Melvin, T.M. and Briffa, K.R., 2008. A "signal-free" approach to dendroclimatic standardisation.Dendrochronologia, 26, 71-86.

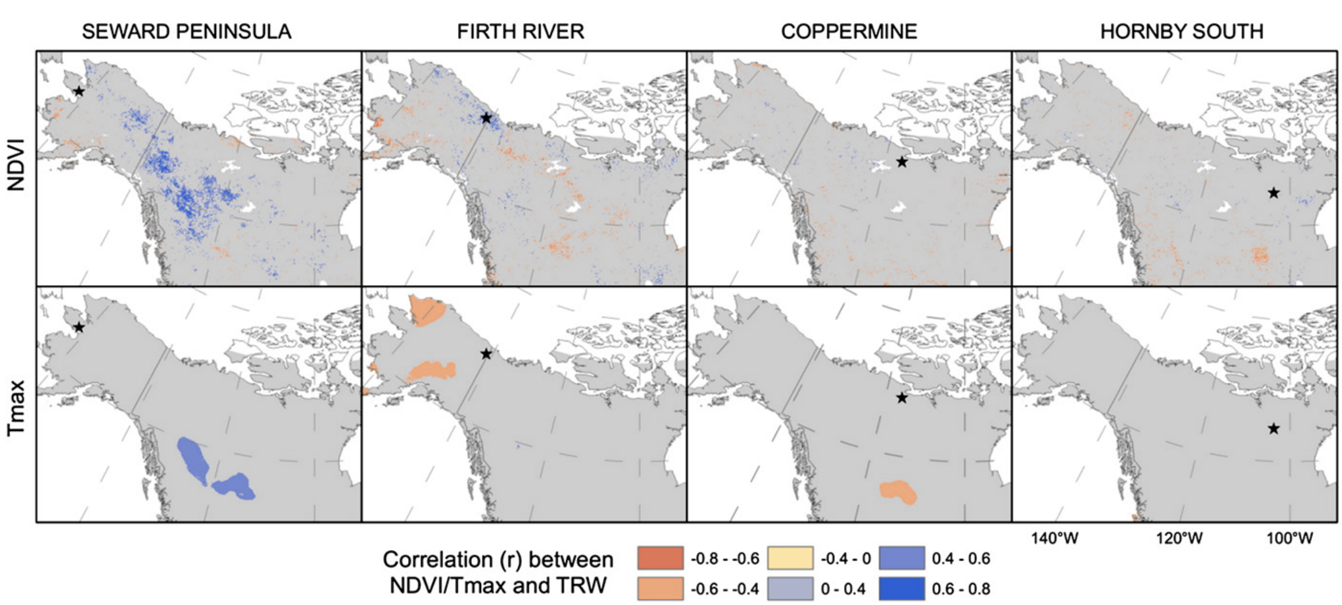

Fig. A.3. Correlation (r) between tree-ring width (TRW) at four sites and (top row) mean daily maximum temperature and (bottom row) GIMMS NDVI in July. Correlations were calculated from time series starting in 1982 and ending between 2001 and 2004 depending on the year of sampling at each site. Gray areas indicate non-significant correlation ($P \geq 0.05$).

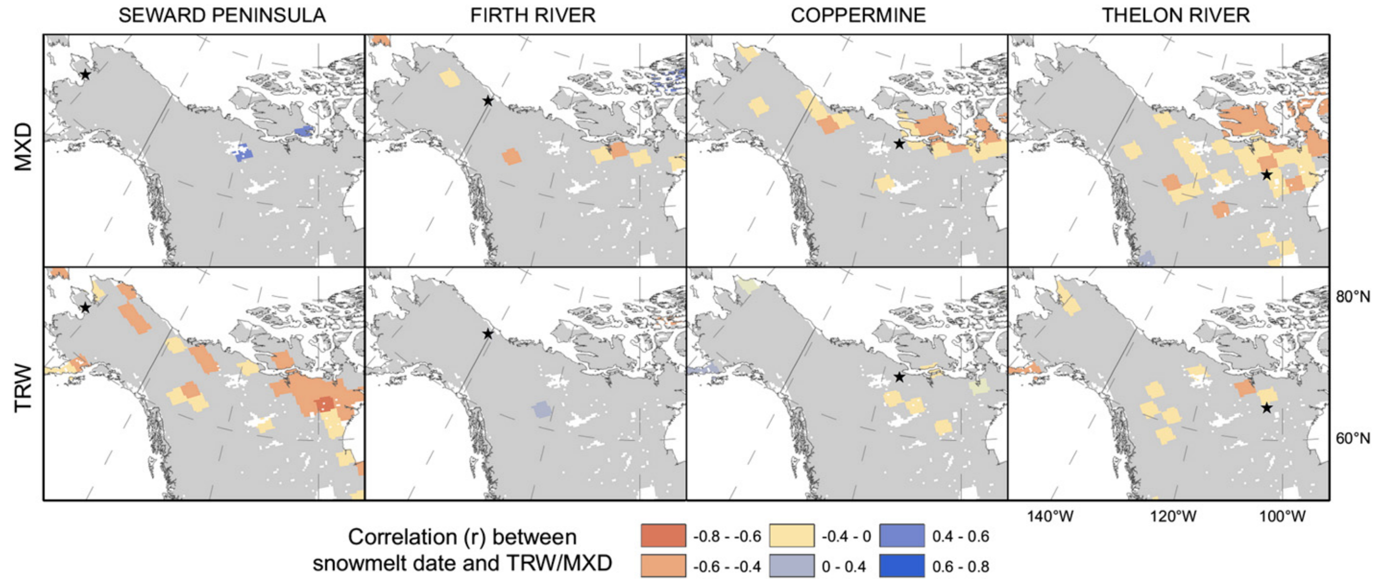

Fig. A.4. Correlation (r) between maximum latewood density (MXD, top row) and tree-ring width (TRW, bottom row) chronologies at four sites indicated by stars and estimated snow melt dates since 1968. Correlations were calculated from time series starting in 1968 and ending between 2001 and 2004 depending on the year of sampling at each site. Gray areas indicate non-significant correlation ($P \geq 0.05$).

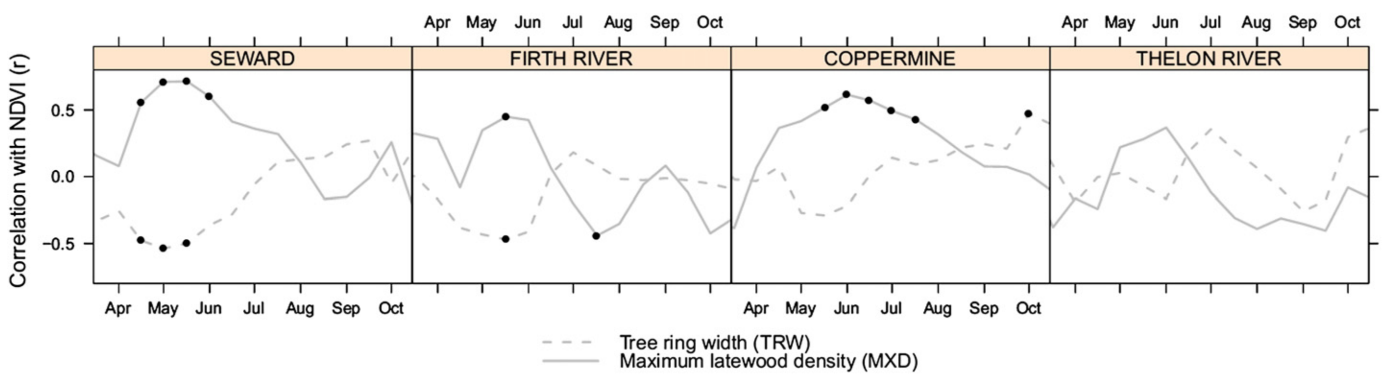

Fig. A.5. Correlation (r) between tree-ring chronologies (ring width and maximum latewood density (MXD)) and corresponding NDVI observations in the forthcoming 3 g version of the GIMMS data set, resampled to monthly resolution and fortnightly frequency. Black dots indicate statistically significant correlation ($P < 0.05$). Correlations were calculated from time series starting in 1982 and ending between 2001 and 2004 depending on the year of sampling at each site.

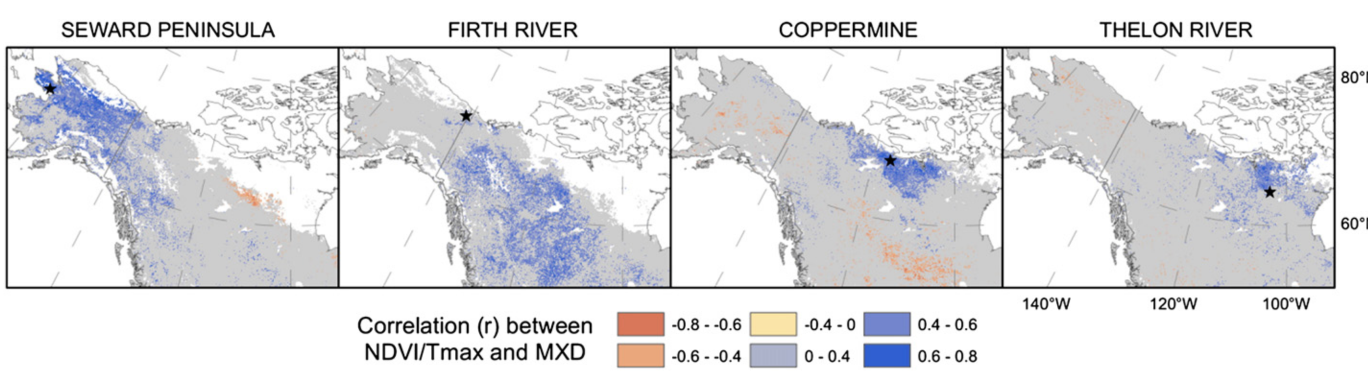

Fig. A.6. Correlation (r) between maximum latewood density (MXD) tree-ring chronologies at four sites indicated by stars and NDVI observations in the forthcoming 3 g version of the GIMMS data set. NDVI in May was used at the Seward Peninsula and Firth River sites, and in June for the Coppermine and Thelon River sites where the growing season starts later. Correlations were calculated from time series starting in 1982 and ending between 2001 and 2004 depending on the year of sampling at each site. Gray areas indicate non-significant correlation ($P \geq 0.05$).

References

ACIA, 2004. Arctic Climate Impact Assessment. Cambridge University Press, Cambridge. (1042 pp.).

Anchukaitis, K.J., et al., in press. Tree-ring reconstructed summer temperatures from northwestern North America during the last nine centuries. Journal of Climate. http://dx.doi.org/10.1175/JCLI-D-11-00139.1.

Andreu-Hayles, L., et al., 2011. Varying northern forest response to arctic environmental change at the Firth River, Alaska. Environmental Research Letters 6 (045503).

Armstrong, R.L., Brodzik, M.J., 2005. Northern Hemisphere EASE-Grid Weekly Snow Cover and Sea Ice Extent Version 3. National Snow and Ice Data Center. Digital media, Boulder, Colorado USA.

Barber, V.A., Juday, G.P., Finney, B.P., 2000. Reduced growth of Alaskan white spruce in the twentieth century from temperature-induced drought stress. Nature 406, 668–673.

Beck, P.S.A., Goetz, S.J., 2011. Satellite observations of high northern latitude vegetation productivity changes between 1982 and 2008: ecological variability and regional differences. Environmental Research Letters 6, 045501.

Beck, P.S.A., et al., 2011a. Changes in forest productivity across Alaska consistent with biome shift. Ecology Letters 14 (4), 373–379.

Beck, H.E., et al., 2011b. Global evaluation of four AVHRR–NDVI data sets: intercomparison and assessment against Landsat imagery. Remote Sensing of Environment 15, 2547–2563.

Bergeron, O., et al., 2007. Comparison of carbon dioxide fluxes over three boreal black spruce forests in Canada. Global Change Biology 13 (1), 89–107.

Berner, L., Beck, P.S.A., Bunn, A., Lloyd, A.H., Goetz, S.J., 2011. Evaluation of high-latitude coniferous forest growth using a satellite-derived spectral vegetation index. Journal of Geophysical Research 116, G01015.

Bonan, G.B., 2008. Forests and climate change: forcings, feedbacks, and the climate benefits of forests. Science 320 (5882), 1444–1449.

Briffa, K.R., Jones, P.D., Schweingruber, F.H., 1992. Tree-ring density reconstructions of summer temperature patterns across western North America since 1600. Journal of Climate 5, 735–754.

Briffa, K.R., Jones, P.D., Schweingruber, F.H., Shiyatov, S.G., Cook, E.R., 1995. Unusual twentieth-century summer warmth in a 1,000-year temperature record from Siberia. Nature 376, 156–159.

Briffa, K.R., et al., 1998a. Trees tell of past climates: but are they speaking less clearly today? Philosophical Transactions of the Royal Society B: Biological Sciences 353, 65–73.

Briffa, K.R., et al., 1998b. Reduced sensitivity of recent tree-growth to temperature at high northern latitudes. Nature 391 (6668), 678–682.

Bronson, D.R., Gower, S.T., Tanner, M., Van Herk, I., 2009. Effect of ecosystem warming on boreal black spruce bud burst and shoot growth. Global Change Biology 15 (6), 1534–1543.

Bunn, A.G., Goetz, S.J., 2006. Trends in satellite-observed circumpolar photosynthetic activity from 1982 to 2003: the influence of seasonality, cover type, and vegetation density. Earth Interactions 10 (12), 1–19.

Cook, E.R., Kairiukstis, L.A. (Eds.), 1990. Methods of Dendrochronology. Applications in the Environmental Sciences. Kluwer, Dordrecht (394 pp.).

Cook, E.R., Peters, K., 1981. The smoothing spline: a new approach to standardizing forest interior tree-ring width series for dendroclimatic studies. Tree-Ring Bulletin 41, 45–53.

Cook, E.R., Peters, K., 1997. Calculating unbiased tree-ring indices for the study of climatic and environmental change. The Holocene 7, 359–368.

D'Arrigo, R.D., Malmstrom, C.M., Jacoby, G.C., Los, S.O., Bunker, D.E., 2000. Correlation between maximum latewood density of annual tree rings and NDVI based estimates of forest productivity. International Journal of Remote Sensing 21 (11), 2329–2336.

D'Arrigo, R., Mashig, E., Frank, D., Jacoby, G., Wilson, R., 2004a. Reconstructed warm season temperatures for Nome, Seward Peninsula, Alaska. Geophysical Research Letters 31, L09202.

D'Arrigo, R.D., et al., 2004b. Thresholds for warming-induced growth decline at elevational tree line in the Yukon Territory, Canada. Global Biogeochemical Cycles 18, GB3021.

D'Arrigo, R., Mashig, E., Frank, D., Wilson, R., Jacoby, G., 2005. Temperature variability over the past millennium inferred from Northwestern Alaska tree rings. Climate Dynamics 24, 227–236.

D'Arrigo, R., Wilson, R., Liepert, B., Cherubini, P., 2008. On the 'Divergence Problem' in Northern Forests: a review of the tree-ring evidence and possible causes. Global and Planetary Change 60 (3–4), 289–305.

D'Arrigo, R., et al., 2009. Tree growth and inferred temperature variability at the North American Arctic treeline. Global and Planetary Change 65 (1–2), 71–82.

Davi, N.K., Jacoby, G.C., Wiles, G.C., 2003. Boreal temperature variability inferred from maximum latewood density and tree-ring width data, Wrangell Mountain region, Alaska. Quaternary Research 60, 252–262.

Dye, G.D., Tucker, C.J., 2003. Seasonality and trends of snow cover, vegetation index and temperature in northern Eurasia. Geophysical Research Letters 30 (7), 1405. http://dx.doi.org/10.1029/2002GL016384.

Esper, J., Frank, D., 2009. Divergence pitfalls in tree-ring research. Climatic Change 94 (3), 261–266. http://dx.doi.org/10.1007/s10584-009-9594-2.

Forbes, B.C., Macias-Fauria, M., Zetterberg, P., 2009. Russian Arctic warming and 'greening' are closely tracked by tundra shrub willows. Global Change Biology 16 (5), 1542–1554. http://dx.doi.org/10.1111/j.1365-2486.2009.02047.x.

Frank, D., Esper, J., 2005. Characterization and climate response patterns of a high-elevation, multi-species tree-ring network in the European Alps. Dendrochronologia 22, 107–121.

Goetz, S.J., Bunn, A.G., Fiske, G.J., Houghton, R.A., 2005. Satellite-observed photosynthetic trends across boreal North America associated with climate and fire disturbance. Proceedings of the National Academy of Sciences of the United States of America 102 (38), 13521–13525.

Helama, S., Lindholm, S., Timonen, M., Eronen, M., 2004. Detection of climate signal in dendrochronological data analysis: a comparison of tree-ring standardization methods. Theoretical and Applied Climatology 79, 239–254.

Jacoby, G.C., D'Arrigo, R.D., 1995. Tree ring width and density evidence of climatic and potential forest change in Alaska. Global Biogeochemical Cycles 9 (2), 227–234.

Juday, G.P., Alix, C., 2012. Consistent negative temperature sensitivity and positive influence of precipitation on growth of floodplain Picea glauca in Interior Alaska. Canadian Journal of Forest Research 42 (3), 561–573.

Kaufmann, R.K., et al., 2004. The effect of growing season and summer greenness on northern forests. Geophysical Research Letters 31, L09205.

Kirdyanov, A.V., Vaganov, E.A., Hughes, M.K., 2007. Separating the climatic signal from tree-ring width and maximum latewood density records. Trees-Structure and Function 21 (1), 37–44.

Lloyd, A.H., Rupp, T.S., Fastie, C.L., Starfield, A.M., 2003. Patterns and dynamics of treeline advance on the Seward Peninsula, Alaska. Journal of Geophysical Research-Atmospheres 108 (D2), 8161.

Lloyd, A.H., Bunn, A.G., Berner, L., 2010. A latitudinal gradient in tree growth response to climate warming in the Siberian taiga. Global Change Biology 17 (5), 1935–1945.

Lucht, W., Schaphoff, S., Erbrecht, T., Heyder, U., Cramer, W., 2006. Terrestrial vegetation redistribution and carbon balance under climate change. Carbon Balance and Management 1. http://dx.doi.org/10.1186/1750-0680-1-6.

MacDonald, G.M., Kremenetski, K.V., Beilman, D.W., 2008. Climate change and the northern Russian treeline zone. Philosophical Transactions of the Royal Society B: Biological Sciences 363 (1501), 2283–2299.

Macias-Fauria, M., Forbes, B.C., Zetterberg, P., Kumpula, T., 2012. Eurasian Arctic greening reveals teleconnections and the potential for structurally novel ecosystems. Nature Climate Change 2, 613–618. http://dx.doi.org/10.1038/nclimate1558.

McKenney, D.W., Pedlar, J.H., Papadopol, P., Hutchinson, M.F., 2006. The development of 1901–2000 historical monthly climate models for Canada and the United States. Agricultural and Forest Meteorology 138 (1–4), 69–81.

Melvin, T.M., Briffa, K.R., 2008. A "signal-free" approach to dendroclimatic standardisation. Dendrochronologia 26, 71–86.

Mitchell, T.D., Jones, P.D., 2005. An improved method of constructing a database of monthly climate observations and associated high-resolution grids. International Journal of Climatology 25 (6), 693–712.

Myneni, R.B., Keeling, C.D., Tucker, C.J., Asrar, G., Nemani, R.R., 1997. Increased plant growth in the northern high latitudes from 1981–1991. Nature 386, 698–702.

Panyushkina, I.P., Hughes, M.K., Vaganov, E.A., Munro, M., 2003. Summer temperature in northeastern Siberia since 1642 reconstructed from tracheid dimensions and cell numbers of *Larix cajanderi*. Canadian Journal of Forest Research 33, 1905–1914.

Pinzon, J.E., Raynolds, M., Pack, E., Tucker, C.J., submitted for publication. Revisiting error, precision and uncertainty in NDVI AVHRR data: development of a consistent NDVI3g time series. Remote Sensing.

Scholze, M., Knorr, W., Arnell, N.W., Prentice, I.C., 2006. A climate-change risk analysis for world ecosystems. Proceedings of the National Academy of Sciences 103 (35), 13116–13120.

Sturm, M., Wagner, A.M., 2010. Using repeated patterns in snow distribution modeling: An Arctic example. Water Resources Research 46, W12549. http://dx.doi.org/10.1029/2010WR009434.

Tucker, C.J., et al., 2005. Extended AVHRR 8-km NDVI data set compatible with MODIS and SPOT vegetation NDVI data. International Journal of Remote Sensing 26, 4485–4498.

Vaganov, E.A., Hughes, M.K., Kirdyanov, A.V., Schweingruber, F.H., Silkin, P.P., 1999. Influence of snowfall and melt timing on tree growth in subarctic Eurasia. Nature 400 (6740), 149–151.

Wilmking, M., Juday, G.P., Barber, V.A., Zald, H.S., 2004. Recent climate warming forces contrasting growth responses of white spruce at treeline in Alaska through temperature thresholds. Global Change Biology 10, 1–13.

Wilmking, M., D'Arrigo, R., Jacoby, G.C., Juday, G.P., 2005. Increased temperature sensitivity and divergent growth trends in circumpolar boreal forests. Geophysical Research Letters 32, L15715.

Yasue, K., Funada, R., Kobayashi, O., Ohtani, J., 2000. The effects of tracheid dimensions on variations in maximum density of *Picea glehnii* and relationships to climatic factors. Trees — Structure and Function 14, 223–229. http://dx.doi.org/10.1007/PL00009766.